

Flexural fatigue behavior of reinforced concrete T-beams strengthened with a composite of prestressed steel wire ropes embedded in polyurethane cement (PSWR-PUC)

Kexin Zhang¹ , Yi Wang¹ , Yiqi Wang², Jiaqi Qiu¹, Longsheng Bao¹, Dianyue Cao¹, Shiyu Chen¹

¹Shenyang Jianzhu University, School of Transportation and Surveying Engineering, No. 25 Hunnan Zhong Road, 110168, Shenyang, China.

²Heilongjiang Institute of Technology, College of Civil and Architectural Engineering, No.999 Hongqi Street, 150050, Harbin, China.

e-mail: jt_zkx@sjzu.edu.cn, 471398766@qq.com, wangyiqihit@163.com, 2458520265@qq.com, baolongsheng710605@163.com, 270959277@qq.com, 1094811632@qq.com

ABSTRACT

To study the fatigue properties of reinforced concrete (RC) T-beams strengthened with a composite of prestressed steel wire ropes embedded in polyurethane cement (PSWR-PUC), which is an innovative reinforcement method, two RC beams without strengthening, three RC beams with a composite of prestressed steel wire ropes embedded in polymer mortar (PSWR-PM) and three RC beams with PSWR-PUC were designed. Some key parameters, such as the material into which the wire rope is imbedded, the fatigue loading, and the tension of steel wire ropes, are discussed. The experimental results show that PSWR-PUC reinforcement can significantly improve the monotonicity and fatigue performance of RC T-beams. The PSWR-PUC strengthening can significantly reduce beam deflection and steel bar stress. Under the same load, the maximum strain and strain range of PSWR-PUC reinforced beams are significantly smaller than those of PSWR-PM reinforced beams. Due to the excellent properties of polyurethane cement composite with high strength, high bond, and high toughness, the cracking and peeling phenomenon of polymer mortar in PSWR-PUC reinforced beams did not occur, which can improve the fatigue life of beams by reducing the stress of steel bars. Due to the cracking, falling off, and peeling of polymer mortar, the bonded prestressed wire rope becomes unbonded pre-stressed wire rope, which redistributes the stress of the beam and further increases the stress of the steel bars.

Keywords: Reinforced concrete (RC) T-beams; Bending fatigue; Polyurethane cement (PUC); PSWR-PUC strengthening technique; Prestressed steel wire rope (PSWR).

1. INTRODUCTION

Due to overload and harsh environmental conditions, reinforced concrete (RC) bridges will degrade with the increase in service life, resulting in a serious shortage of bridge bearing capacity. There is a need to employ suitable materials and technologies to strengthen these bridges and extend their service life. Polyurethane cement (PUC) is applied and is becoming an attractive solution for strengthening/retrofitting the RC structures [1–3]. Generally, compared with traditional repair materials such as FRP, PUC can not only adapt to the uneven surface of bridge concrete but also quickly restore traffic. The PUC material is made of polyurethane and Portland cement, which has the characteristics of lightweight, high strength, high toughness, and corrosion resistance [2–4]. In addition, PUC materials have good bonding properties and bond firmly to concrete without the need for additional adhesives, which is considered a potential repair material by many scholars [5, 6].

HUSSAIN *et al.* [2] and ZHANG and SUN [7] carried out reinforcement tests of scale model beams and load tests of actual bridge reinforcement. The results show that the flexural strength, stiffness, and other bearing capacity of the repaired bridge are improved. PUC materials can greatly limit the development of cracks and improve the durability of the reinforced structure. ZHANG and SUN [8, 9] used wire mesh-polyurethane cement (WM-PUC) composites to strengthen RC beams and compared them with ferrocement reinforced beams. It found that the ultimate load of the WM-PUC reinforced beam with four layers of wire mesh is 43.8% higher than that of the corresponding reinforced beam with ferrocement. These two reinforcement methods, PUC and WM-PUC, as well as the commonly used bonding steel plate and bonding carbon-fiber-reinforced polymer (CFRP) sheet method, are all considered passive reinforcement techniques. WU *et al.* [10, 11]

conducted an experimental study on the reinforcement of RC beams with prestressed steel wire rope-polymer mortar (PSWR-PM) and compared the experimental results with those of CFRP beams strengthened with PWSR-PM. It can be shown that PSWR-PM can significantly improve the stiffness and bearing capacity of RC beams. However, the debonding failure of reinforced layers and cracks usually occur in the rehabilitation of RC members with PSWR-PM, which seriously affects the durability of the reinforced structure and steel strands [12, 13]. In addition, the fatigue test of RC beams strengthened with PSWR-PM surface layer is carried out by LIU *et al.* [14] and HUANG *et al.* [12], and the influence of parameters such as interface condition, prestress level, and anchoring mode on the flexural fatigue performance of reinforced specimens were emphatically studied. For the reinforcement members with end anchorage, the interface bonding performance of the reinforcement layer lacks stability, and the bonding anchorage failure is easy to occurs, which reduces the reinforcement effect. The performance of the reinforcement parts with interface defects is comparable to that of the contrast parts. The interface between the reinforced layer mortar and the bulk beam is the weakest link of the reinforced concrete beam with high strength steel wire ropes.

In order to solve the durability problem caused by cracking and dropping of polymer mortar in PSWR-PM composite reinforcement, ZHANG *et al.* [8, 15, 16] propose an innovative RC bridge strengthening technique, a composite of PSWRs embedded in PUC (PSWR-PUC). PUC not only improves prestressed steel wire rope durability and anchorage safety but also provides additional reinforcement to the beam [16]. Compared with the PSWR-PM reinforced beam, the strength, stiffness, and crack restraint ability of the PSWR-PUC reinforced beam are significantly improved [8, 9]. Compared with PSWR-PM reinforced beams, the reinforcement layer of PSWR-PUC reinforced beams will not peel off, solving the problem of poor bonding and anchoring performance of the reinforcement layer of PSWR-PM reinforced beams. Compared with ordinary asphalt concrete, polyurethane cement has better fatigue performance [6]. In addition, accelerated aging and wear tests showed that the composite had good UV resistance and mechanical stability [10, 17–19].

Although the PSWR-PUC technology can significantly improve the static performance of beams, the fatigue performance of the PSWR-PUC strengthening is an important consideration, which directly affects the operation of the main girder. This paper presents the results of experimental studies on the fatigue behavior of RC T-beams strengthened with PSWR-PUC, which include two unstrengthened beams, three PSWR-PUC-strengthened beams, and three PSWR-PM-strengthened beams. The main variable parameters were the material into which the wire rope was embedded, the fatigue loading, and the tension of steel wire ropes. Through the fatigue tests of PSWR-PUC and PSWR-PM reinforced beams, the effects of two different reinforcement techniques on the bending fatigue properties of beams were compared, and the mechanical behaviors of undamaged beams after 2 million cycles of loading were tested by monotone loading.

2. TEST PROGRAMME

2.1. Material properties

The compressive strength of the RC beam at 28-day age was 43.3 MPa, and the elastic modulus was approximately 35 GPa, according to the standard test method (JTG E30-2005) [20]. The diameter of the longitudinal tensile steel bar used in the beam is 20 mm, and its measured yield strength is 418 MPa. The diameter of the stirrup is 8 mm, and the spacing is 100 mm. The elastic modulus of all steel bar was 200 GPa. According to the Chinese national standard [19], the average compressive strength of polymer mortar at 28-day age was 55 MPa, the average flexural strength was 5.8 MPa, and the elastic modulus was 23.1 GPa. The PUC composite material is polymerized from polyisocyanate, polyether polyol, and cement [2, 3, 15–18]. The ordinary Portland cement used in this study was produced by Dalian Oda Cement Co., LTD., and its free moisture was removed by oven heating. The polyisocyanate was produced by Basf (China) Co. LTD. Shanghai Branch, the full name is 4,4'-diphenylmethane diisocyanate, and its content is not less than 98%. The polyol, produced by Linuo Chemical Group Co., Ltd. in Zibo of Shandong Province, has a molecular weight of 7000 and a water content of less than 0.1%. The mixing ratio of the PUC composite adopts a mass ratio (cement: polyol: polyisocyanate = 2:1:1). The density of the PUC composite material measured was 1550 kg/m³. The bending tensile strain-stress curves are shown in Figure 1. As shown in Table 1, the bending properties of PUC are considered in terms of ultimate bending strength, modulus of elasticity under bending performance, and maximum strain during bending, and the compressive properties of PUC are considered in terms of ultimate compressive strength, modulus of elasticity under compressive performance and maximum strain during compression. The diameter of the wire rope was 4 mm, the cross-sectional area was 10.55 mm². It has the characteristics of high strength, low creep rate, and good ductility. The steel wire rope had an ultimate tensile stress of 1200 MPa, an ultimate tensile strain of 0.02, and a Young's modulus of 130 GPa.

PUC was made into 100 × 100 × 100 mm³ cube test blocks and 100 × 100 × 400 mm³ prism test blocks. The regimen temperature was 20 ± 2°C, and the regimen time was 28-day age. The compressive strength and

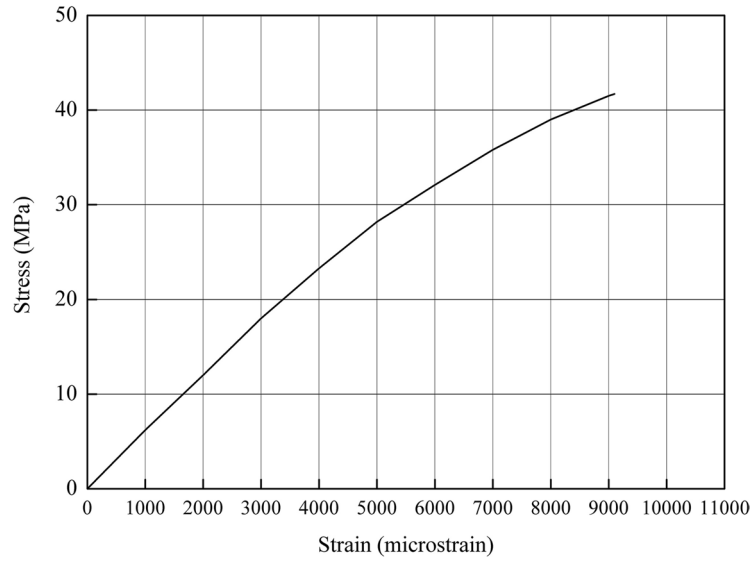


Figure 1: Flexural stress-strain curve of the PUC composite.

Table 1: Bending and compressive properties of the PUC material.

| BENDING PROPERTIES | | | COMPRESSIVE PROPERTIES | | |
|---------------------------------|-----------------------------|------------------------|-------------------------------------|-----------------------------|------------------------|
| Ultimate bending strength (MPa) | Modulus of elasticity (MPa) | Maximum strain (mm/mm) | Ultimate compressive strength (MPa) | Modulus of elasticity (MPa) | Maximum strain (mm/mm) |
| 41.5 | 5500 | 0.009 | 65 | 6200 | 0.04 |

flexural strength tests of PUC material were conducted based on the Test Methods of Cement and Concrete for Highway Engineering [21]. The average compressive strength was 65 MPa, and the flexural strength was 41.5 MPa.

2.2. Test scheme and specimen configuration

In order to investigate the effects of PUC and PM on the fatigue performance of PSWR reinforced beams, experimental research was conducted on the mechanical properties of the materials first. Considering the good adhesion between concrete and PUC and PM, the specific testing plan is as follows. In this test, eight RC beams were constructed. The study prepared eight RC T-beam specimens. The dimensions of the T-beam were 400 mm wide \times 320 mm high \times 3000 mm long. Beams B1 and PLCB were unstrengthened beams, beams PLB1 and PLB3 were strengthened with PSWR-PM, and the remaining beams were strengthened with PSWR-PUC. The longitudinal reinforcement diagram and cross-sectional reinforcement diagram are shown in Figures 2 and 3. The eight beams have the same geometric shape, and their reinforcement details are shown in Table 2. Beams

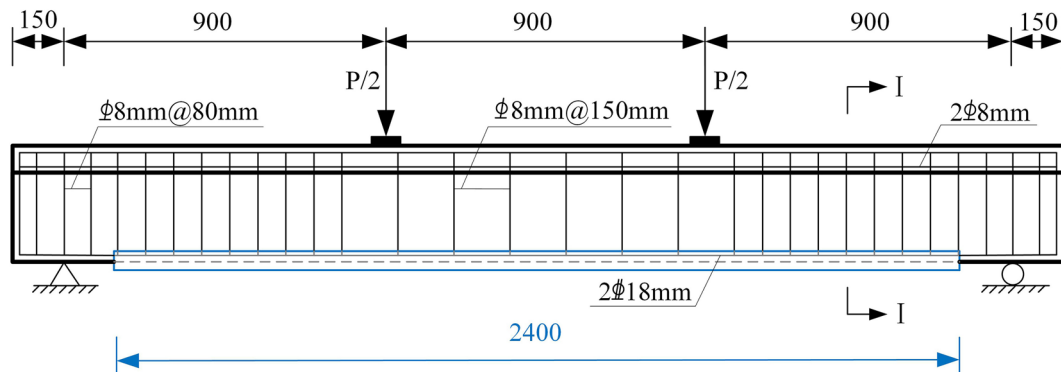
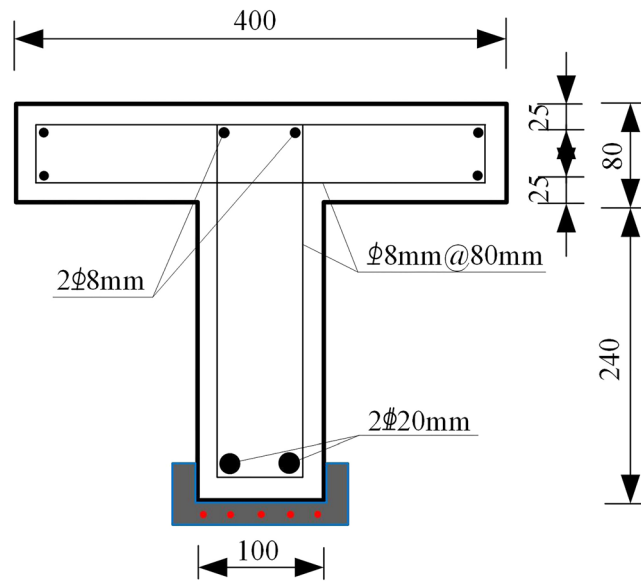


Figure 2: Longitudinal reinforcement diagram of the beam (units: mm).

Table 2: Details of the T-beam specimens.

| GROUP | NOTATION | NUMBER OF WIRE ROPES | PRESTRESSING VALUE | EMBEDDING MATERIAL | MINIMUM LOAD (kN) | MAXIMUM LOAD (kN) | NUMBER OF CYCLES |
|---------------------|----------|----------------------|--------------------|--------------------|-------------------|-------------------|---------------------|
| Monotonic load test | B1 | — | — | — | — | — | |
| | B2 | 5 | 700 | polymer mortar | — | — | |
| | B3 | 5 | 700 | PUC | — | — | |
| Fatigue specimens | PLCB | — | — | — | 30 | 70 | 6.26×10^5 |
| | PLB1 | 5 | 700 | polymer mortar | 30 | 70 | 1.323×10^6 |
| | PLB2 | 5 | 700 | PUC | 15 | 55 | 1×10^6 |
| | | | | | 30 | 70 | 2×10^6 |
| | PLB3 | 7 | 900 | polymer mortar | 45 | 95 | 6.66×10^5 |
| | PLB4 | 5 | 700 | PUC | 45 | 95 | 2×10^6 |

**Figure 3:** Cross-sectional reinforcement diagram of the beam (units: mm).

B1, B2, and B3 are monotonic loading test beams, which are unreinforced, PSWR-PM reinforced and PSWR-PUC reinforced, respectively. According to the test data of the monotonic loading beam, the maximum load and load amplitude of fatigue loading are determined. The beams PLB1, PLB2, and PLB4 are reinforced by five prestressed steel wire ropes, the tensile stress is 700 MPa, and the pouring thickness of PUC material is 25 mm. The PLB3 beam is reinforced by seven prestressed steel wires with a tensile stress of 900 MPa, which is different from that of other beams.

2.3. Strengthening beams with PSWR-PUC

The operation procedure of PSWR-PUC strengthening technology is shown in Figure 4.

Concrete surface preparation: In order to make the concrete surface bond reliably, the bonded surface of all the concrete beams is chiseled manually with a chisel hammer, and the coarse aggregate is leaked (Figure 4(a)).

Tensioning and anchoring the prestressed wire rope: Two grooves with a width of 100 mm were cut at each end of the beam, and anchors were welded to longitudinal steel bars. Each anchorage is similar to a button-hole anchorage, and the wire rope length is calculated according to the design tensile strength. The wire ropes are tensioned and anchored to the beam's end (Figure 4(b)).

Fixing wood template and casting the PUC material: A wooden template was erected at the bottom of the beam. The PUC material is stirred for 3 min and poured into the pre-set template (Figure 4(c) and (d)).

Removing the template: The wood template was removed after 1d (Figure 4(e)).



Figure 4: Operation procedure of PSWR-PUC reinforced beams: (a) concrete surface preparation, (b) tensioning and anchoring the prestressed wire rope, (c) fixing wood template and casting the PUC material, (d) Mixing and stirring the PUC material, (e) Removing the wood template.

2.4. Fatigue loading scheme

Based on the specifications of Steel Strand for Prestressed Concrete (GB/T 5224-2023), Test Methods for Steel for Prestressed Concrete (GB/T 21839-2019), and Code for Acceptance of Construction Quality of Concrete Structures (GB 50204-2015), fatigue tests were conducted using a four-point loading method [22–24]. The distance between the two loading points in the span of the test beam is 900 mm, and the beam body is placed on two steel support piers. The loading diagram is shown in Figure 5. The fatigue test adopts constant amplitude fatigue loading mode, and the loading frequency is about 5 Hz. The PLS-500 electro-hydraulic servo fatigue test system produced by Jinan East Test Company was used for fatigue test. The maximum load value of the actuator was 500 kN, and the maximum stroke was ± 150 mm, which could meet the loading requirements of the fatigue test. The testing machine is composed of a hydraulic pulsator, a control system, and a hydraulic loading pulsator. The load generated by the actuator is transferred to the cushion block on the surface of the beam body through the distribution beam. The fatigue test is preceded by a static load test at an appropriate load in order to check whether the instrument is working properly. During the fatigue test, the dynamic strain

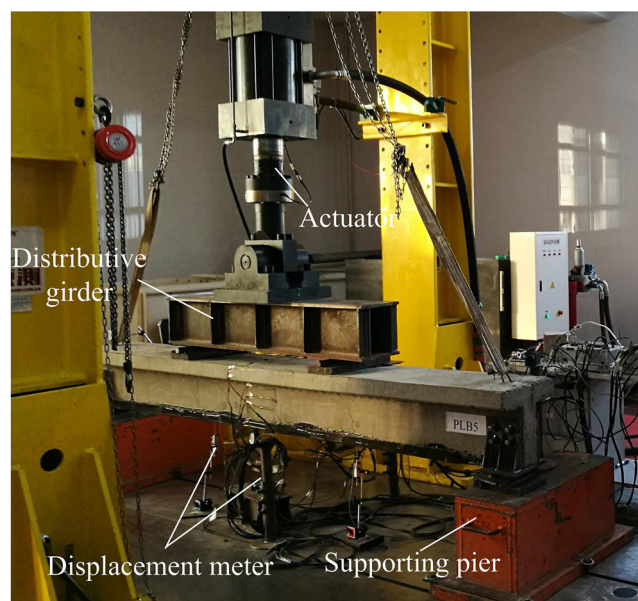


Figure 5: Fatigue test diagram.

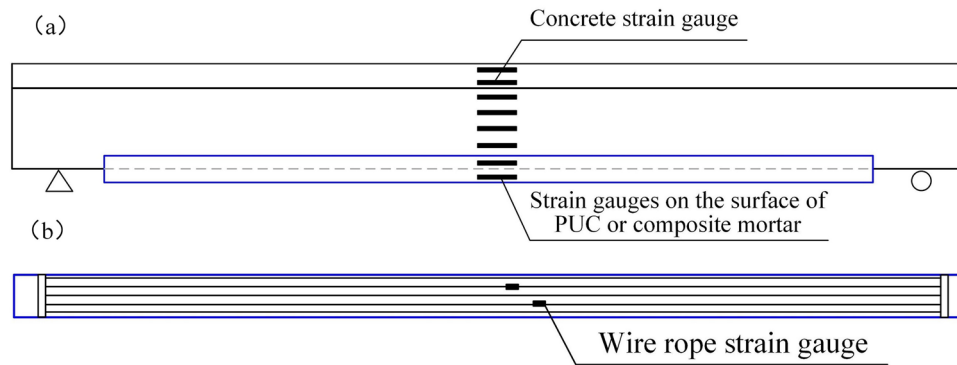


Figure 6: Specimen measuring point layout.

Table 3: Static load test results.

| BEAM NUMBER | CRACK LOAD (kN) | YIELD LOAD (kN) | ULTIMATE LOAD (kN) | MAXIMUM STRAIN OF PUC ($\mu\epsilon$) | MAXIMUM STRAIN OF COMPOSITE MORTAR ($\mu\epsilon$) | MAXIMUM STRAIN OF STEEL WIRE ROPE ($\mu\epsilon$) |
|-------------|-----------------|-----------------|--------------------|---|--|---|
| B1 | 22 | 77 | 102 | — | — | — |
| B2 | 38 | 98 | 143 | — | 556 | 10790 |
| B3 | 46 | 122 | 206 | 7439 | — | 11168 |

and dynamic deflection test parameters were collected respectively. When the test load reached 10,000, 20,000, 50,000, 100,000, 200,000, 500,000, 1,000,000, 1.5 million, and 2,000,000 times, the machine was stopped and unloaded to zero, and a cyclic static load test was carried out. Strains were recorded for concrete, reinforcement, steel wire rope, polyurethane grout, and mortar; beam deflections, crack lengths, and maximum crack widths were also monitored. The failure characteristics, fatigue loading times, and load values at the time of failure were recorded. The fatigue loading of the component is set as the target of 2,000,000 times. Assuming that there is no damage after 2,000,000 times, stop the machine and do the static load failure test.

In order to prevent sliding of the test beam during fatigue loading, steel hoop bearings were made to prevent sliding. The steel support pier is fixed on the rigid ground by steel plate layering to prevent the support pier from sliding in the process of vibration.

2.5. Measurement point layout and test content

The measurement of the test is mainly divided into two parts: one part is the strain measurement of materials under load, including steel bar, concrete, PUC material, polymer mortar and steel wire rope, and the other part is the deformation measurement of components. The concrete strain measurement mainly consists of 120 Ω resistance strain gauges. Six 100 mm \times 3 mm strain gauges are uniformly arranged along the section height in the middle of the beam span to observe the concrete strain distribution along the section height and verify whether the plane assumption is established. Among them, four and two strain gauges are arranged on the beam ribs and flanges respectively. Two 100 mm \times 3 mm strain gauges were pasted on the side and bottom of PUC or PM to observe the strain changes of the material. Four 5 mm \times 3 mm strain gauges are pasted on the two tensile rebar, which are respectively arranged at the loading point and the mid-span position. Two steel wire ropes were selected and a strain gauge of 3 mm \times 2 mm was arranged in the loading area of the pure bending section respectively. The strain gauge of the two steel wire ropes should be stagger arranged to avoid being on the same cross-section. The specific strain measurement layout is shown in Figure 6.

Static load test includes three specimens: B1, B2 and B3. The main test results of each specimen are shown in Table 3, in which the steel wire rope, PUC and PM strain are the actual measured results.

3. MONOTONIC LOAD TEST

The load-deflection curves of all specimens are shown in Figure 7. It can be seen that the cracking load of the unstrengthened beam is smaller than that of the strengthened B1 beam. After section cracking, the stiffness of the

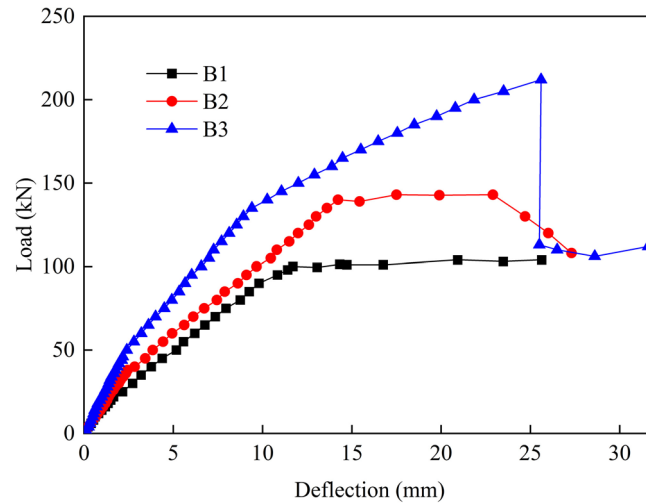


Figure 7: Load-deflection curve under monotonic load.

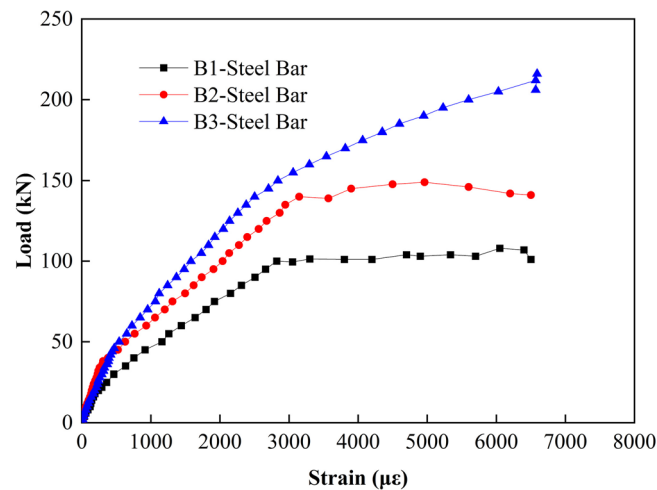


Figure 8: Load-strain of steel bar monotonic load.

strengthened beam decreases and the cracks rapidly develop in the vicinity of the flange plate. When it reaches 76 kN, the deflection of the beam increases sharply because the reinforcement of the specimen reaches the yield point, and then the load-deflection curve is close to the level.

The cracking load of beam B2 strengthened with PSWR-PM is larger than that of the contrast specimen, and the slope of the curve before cracking is slightly higher than that of the unreinforced beam. After cracking, the section stiffness of the specimen is obviously weakened as compared with that of the specimen. The section reinforcement caused by the prestressed steel wire rope was increased, so the slope of the curve at this stage was slightly greater than that of the contrast specimen B1. When the load reached around 98 kN, the steel bars of beam B2 began to yield, and the steel wire ropes continued to play a tensile role. With the increase of deformation, the bearing capacity of the specimen continued to rise, and the slope of the load-deflection curve of beam B2 was significantly higher than that of the contrast specimen B1. When the load rises to 102 kN, the load-deflection curve approaches the level and the prestressed wire rope yields.

Under the same wire rope arrangement condition, the prestressed wire rope of beam B3 is embedded in polyurethane cement material, and the cracking load and yield load of this specimen are significantly increased compared with the unreinforced beam B1 and the PSWR-PUC-strengthened-beam B2. It can be seen from the curve that the slope of the load-deflection curve of specimen B3 before cracking is close to that of specimens B1 and B2. However, the distance between B3 B1, and B2 rapidly widens after cracking. Especially after the reinforcement yield, the prestressed steel wire ropes and PUC play a tensile role, and the load still increases with

the increase of deformation, but the slope of the curve decreases significantly. After the prestressed steel wire ropes yield, the PUC material still plays a tensile role, and the load still rises with the increase of deformation until the composite of steel wire ropes and PUC is broken and destroyed. The load-steel bar strain curves of each specimen are shown in Figure 8. Compared with the contrast beam B1, the steel wire rope in beam B2 can well reduce the strain of the steel bar. Due to the action of polyurethane cement material, beam B3 can better reduce the strain of steel bar than beam B2, which leads to the increase of yield load of beam B3.

4. FATIGUE LOAD TEST

4.1. Observed behavior

The upper and lower limits of fatigue loads of beams PLCB, PLB1 and PLB2 are the same. The maximum value P_{max} of fatigue load is 70 kN, and the minimum value P_{min} is 20 kN, as shown in Table 2. The PLCB beam is subjected to a monotonic loading test, and the maximum load is 70 kN, the upper limit of fatigue load ($0.686P_{u1}$, P_{u1} is the ultimate load value of beam B1), and then relevant test parameters were collected. Under the action of fatigue load, cracks of beam PLCB expand rapidly and extend upward. Figure 9. shows the curve of midspan deflection and cycle times of beam PLCB. After the first 10,000 cycles, the midspan deflection of beam PLCB increases significantly, indicating that the damage accumulation is caused by cyclic load. During the subsequent loading cycles of 10,000 to 20,000 times, the deflection of the beam decreased slightly and then increased steadily to 500,000 times. However, after cyclic loading of 500,000 times, the width of the main crack in the middle span of the beam PLCB reaches 1.5mm, at which point the reinforcement may break or fail, causing the strain reading to terminate. At 626,000 times, the steel bar in the middle span broke, and then the crack extended to the top of the beam, leading to the fracture of the entire beam, as shown in Figure 9.

The upper and lower fatigue limits of beam PLB1 are the same as those of beam PLCB. The PLB1 beam is subjected to a monotonic loading test, and the maximum load is 70 kN, and several vertical cracks appear in the polymer mortar along with the concrete cracking. At this time, the strain of the steel bar is 1147 microstrain, which is 63.8% of the control beam PLCB. Under the action of fatigue load, the crack width is about 0.2 mm when the number of cycles is 200,000. The width of one crack in the span is significantly larger than the other cracks and becomes the main crack. When the cycle reached 1,000,000 times, the polymer mortar surface appeared obvious mesh cracks, and the reinforcement layer and the concrete surface appeared peeling cracks, as shown in Figure 10(a) and (b). However, when the fatigue cycle reached 1,553,000 times, the beam made a sound, and the main steel bar at the bottom was broken. After 3 minutes, the five steel wires in the middle of the span were broken with a loud noise, the whole beam was broken into two sections, and the specimen was destroyed, as shown in Figure 10(c).

4.1.1. Comparison of fatigue performance between beam PLB2 and beam PLB1

The improper hoisting of beam PLB2 during transportation caused several cracks in the middle of the beam body. Without treatment, the PSWR-PUC reinforcement was carried out directly. Therefore, in the initial stage, the upper limit of the fatigue load of beam PLB2 was reduced to 55 kN, and the load

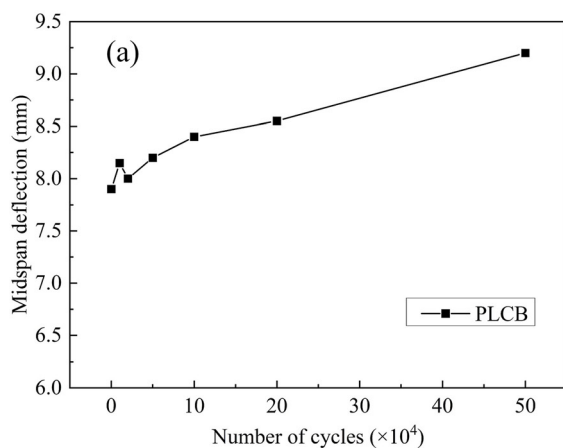


Figure 9: Failure mode of beam PLCB under fatigue load. (a) Curve of midspan deflection and number of cycles; (b) Steel bar fracture diagram of the beam PLCB.



Figure 10: Midspan deflection and failure mode of beam PLB1 under fatigue load. (a) Cracking of polymer mortar; (b) Interlayer stripping of polymer mortar; (c) Steel bar fracture diagram of the beam PLB1.

amplitude was kept unchanged. The fatigue properties of beam PLB2 and beam PLB1 were compared. Beam PLB2 has a mid-span deflection of 5.3 mm under the maximum load in the first cycle, which is significantly larger than the 3.4 mm deflection of beam B1 under the same load. This also indicates that the initial damage significantly affects the initial behavior of beam PLB2. However, during the first 1,000,000 cycles, the deflection of beam PLB2 was not consistently larger than that of beam PLB1. The upper and lower fatigue limits of beam PLB2 are the same as those of beam PLB1. The PLB2 beam is subjected to a monotonic loading test, and the maximum load is 70 kN, and the maximum crack width is 0.10 mm. At this time, the strain of the steel bar is 740 microstrain, which is 41.6% of the control beam PLCB. A fatigue load is applied to beam PLB2. Under the action of fatigue load, concrete cracks

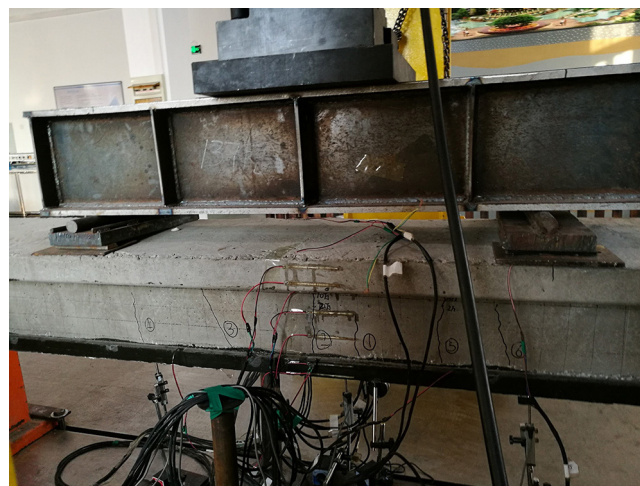


Figure 11: Fatigue failure diagram of beam PLB2.



Figure 12: Fatigue failure diagram of beam PLB3.



Figure 13: Fatigue failure diagram of beam PLB4.

develop rapidly, and the cumulative damage of specimens does not change significantly after the load cycle reaches 200,000 times. The beam PLB2 was loaded for 2,000,000 cycles and still did not fail. Static loading was carried out on the specimen after cyclic loading until the specimen failed. The broken beam after the static load test is shown in Figure 11.

4.1.2. Comparison of fatigue performance between beam PLB3 and beam PLB4

When the upper and lower limits of fatigue loads are 70 kN and 20 kN, the two reinforced beams PLB1 and PLB2 have a large fatigue life. In order to further study the fatigue performance of different embedded materials, the upper limit value and load amplitude value of fatigue load are further increased. The maximum value of fatigue load P_{max} of beam PLB3 and PLB4 is 102 kN, and the minimum value P_{min} is 32 kN. In the static loading process, multiple vertical cracks appear along with the concrete in the polymer mortar of beam PLB3, and the cracks are concentrated in the pure bending section. The crack width of the beam body is about 0.18 mm. After unloading, the concrete cracks of the beam are closed, while the mortar cracks of the reinforcement layer are not completely closed, and the crack width is 0.03 mm. After 200,000 fatigue loads were applied, a crack in the middle of the span became wider and longer, and finally developed into the later main crack. At the same time, obvious mesh cracks appeared on the surface of the polymer mortar, and spalling cracks appeared on the surface of the reinforcement layer and concrete, which were also observed in the cyclic loading process of beam PLB1. During the fatigue loading, obvious horizontal cracks were found between the reinforced layer and the beam body. After half a million times of vibration, the vertical main crack in the span becomes wider. When the vibration reached 660,000 times, with a loud noise, five steel wires in the span broke, and the whole beam was completely destroyed. The damaged beam PLB3 is shown in Figure 12.

The fatigue load value of beam PLB4 is the same as that of beam PLB3. After one million times of fatigue loading, cracks are distributed along the whole length of the beam, and the development of cracks is not obvious. After cyclic loading 2 million times, the beam is not damaged, the polyurethane cement is not broken, and the separation between the polyurethane cement and the concrete has not occurred, as shown in Figure 13.

4.2. Deflection

4.2.1. Comparison of deflection

Figure 14 depicts the relationship between the mid-span deflection of a reinforced beam under fatigue load and the number of cycles. The experimental results show that compared with PSWR-PM reinforcement (beams PLB1 and PLB3), PSWR-PUC reinforcement (beams PLB2 and PLB4) significantly improves the flexural performance of the beam. When the maximum is 70 kN, the midspan deflection of beam PLB1 is 5.66 mm in the first loading cycle, and the midspan deflection increases significantly with the increase of the cycles. In contrast, at a maximum load of 55 kN, beam PLB2 exhibits a smaller deflection than beam RF during the first 1,000,000 loading cycles. Although the load is increased to 70 kN, the deflection of beam PLB2 in subsequent loading is still smaller than that of beam PLB1 after 2,000,000 cycles. Moreover, except for a large increase during the first 20,000 cycles, the maximum deflection of the beam PLB2 remains stable for most of its fatigue life. Under cyclic loading conditions, the deflection of beam PLB1 has a significant development. Due to negligence, midspan deflection and material strain were not recorded when the maximum load was increased to 70 kN. The deflection of beam PLB4 was slightly smaller than that of beam PLB1 before 500,000 cycles. However, due to the large upper limit and amplitude of the fatigue load of beam PLB4, the deformation increases rapidly after 500,000 cycles, exceeding the maximum deflection of beam PLB1. However, during the fatigue test, the deflection of beam PLB1 still increases, while the deflection of beam PLB4 remains stable. Under the maximum load, the mid-span deflection of beam PLB3 is always greater than that of beam PLB4. Similar to beam PLB1, the deflection of beam PLB3 increases continuously during fatigue loading until it fails.

4.2.2. Stiffness comparison

Figure 15 depicts the relationship between the stiffness and the cycle times of beams PLB1, PLB2, PLB3, and PLB4 when the load is 55 kN (maximum load of beam PLB1 for the first 1,000,000 cycles). As can be seen from Figure 15, after 10,000 cycles, the stiffness of PLB1 and PLB3 beams decreased sharply. In subsequent cyclic loading, the stiffness of beams continued to decrease until failure. This suggests that the circulation is causing cumulative damage. Similarly, it is observed that during the first 100,000 cycles, the stiffness of the PLB2 beam decreases and the corresponding deflection increase is evident. However, before 1 million cycles, the stiffness of the PLB1 beam remained basically unchanged. After 1,000,000 cycles, the load was increased to 70 kN. It is observed that the stiffness of beam PLB2 decreases significantly between 1,000,000 and 1,500,000 cycles. The stiffness of the beam PLB2 remained almost constant during the last 1,500,000 cycles of loading, indicating that no significant damage accumulation occurred during this period. In the first

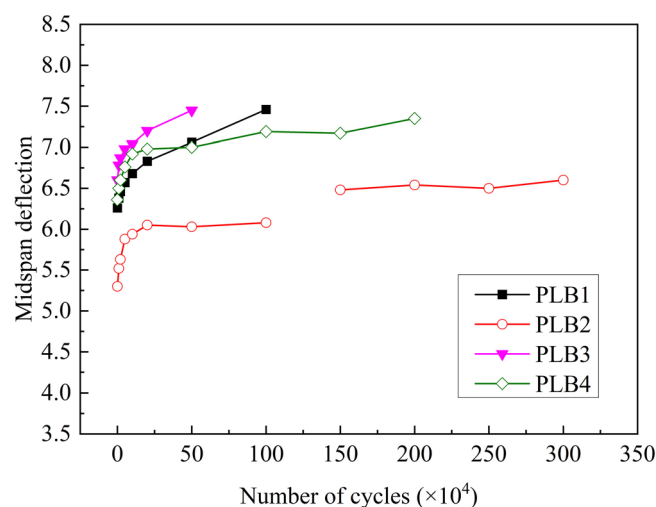


Figure 14: Comparison of midspan deflection.

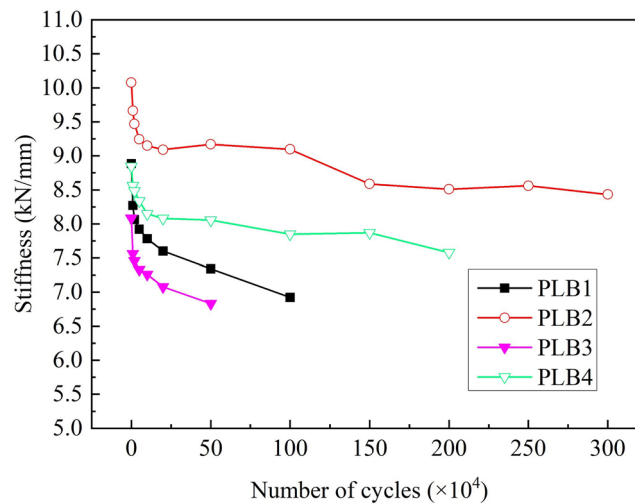


Figure15: Comparison of stiffness of reinforced specimens of reinforced specimens.

100,000 cycles, the stiffness of beam PLB4 decreased, indicating that there was damage accumulation in the beam under cyclic load. However, over the next 1,500,000 cycles, the stiffness of the beam remains almost constant. Between 1,500,000 cycles and 2,000,000 cycles, the stiffness of beam PLB4 decreased significantly, and the corresponding deflection increased, indicating that obvious damage accumulation occurred in the beam during this process.

4.3. Strain of material

Figure 16 shows the strain of the steel bar, steel wire rope, and PUC in the midspan of the beam under different cycles. As shown in Figure 16(a), at the initial loading stage, with the increase in fatigue times, the strain of the steel bar is smaller than that of the wire rope. When the fatigue cycle is more than 100,000 times, the strain of the steel bar increases rapidly and exceeds the strain value of the wire rope due to the cracking and stripping failure of the polymer mortar. As shown in Figure 16(b)–(d), during the whole fatigue cycle, the variation trends of steel bar strain, steel wire rope strain, and PUC material strain are consistent, which indicates that PUC material does not have cracking and peeling failure. On the contrary, PLB1 beams showed a tendency to be uncoordinated between 200,000 and 1,000,000 cycles (Figure 16(a)). As the strain of the steel bar increased, the strain of the wire rope decreased, and eventually, the strain of the steel bar increased more than that of the wire rope, indicating that the bond between the wire rope and the concrete was deteriorating, which was also evidenced by the peeling of the polymer mortar and the cracking of the mesh after 1,000,000 cycles. The variation of the strain of the steel bar and steel wire rope of beam PLB1 also occurs on beam PLB3. Beam PLB3 showed a tendency to be uncoordinated between 100,000 and 500,000 cycles (Figure 16(c)). The strain of the steel bar increases obviously, accompanied by the decrease of the strain of steel wire rope. Similarly, this result also means that the polymer mortar layer has been stripped and cracked.

The strain range of steel bars under different cycles is shown in Figure 16(e). The steel strain of beam PLB2 is lower than that of beam PLB1, although the upper limit and amplitude of the later 2,000,000 cycles load are the same as beam PLB1. The load applied on beam PLB4 is 1.36 times that of beam PLB1, and the initial stress of reinforcement in the two beams is almost the same at the initial loading. With the increase of the number of cycles, due to the peeling and cracking of the polymer mortar layer of beam PLB1, the stress in the beam is redistributed, resulting in the constant increase of the steel bar of beam PLB1, while the steel bar strain range of beam PLB4 remains unchanged. At 1,000,000 cycles, the strain of steel bars of beam PLB4 is 20% lower than that of beam PLB4. The beam PLB1 failed after 1,323,000 cycles, while the beam PLB4 remained intact after 2,000,000 cycles. We believe that the PSWR-PUC reinforcement technology can significantly improve the fatigue life of the beam by reducing the stress level of the steel bar.

The comparison of the strain range of wire rope under different cycles is shown in Figure 16(f). Due to the excellent characteristics of high strength, high bond, and high toughness of polyurethane cement composite, the cracking and peeling phenomenon of PSWR-PUC reinforced beam did not occur, and the strain range of steel wire rope remained unchanged. When beam PLB1 loading cycles exceed 200,000 times and beam PLB3 loading cycles exceed 100,000 times, the strain range of wire rope in the polymer mortar reinforced layer gradu-

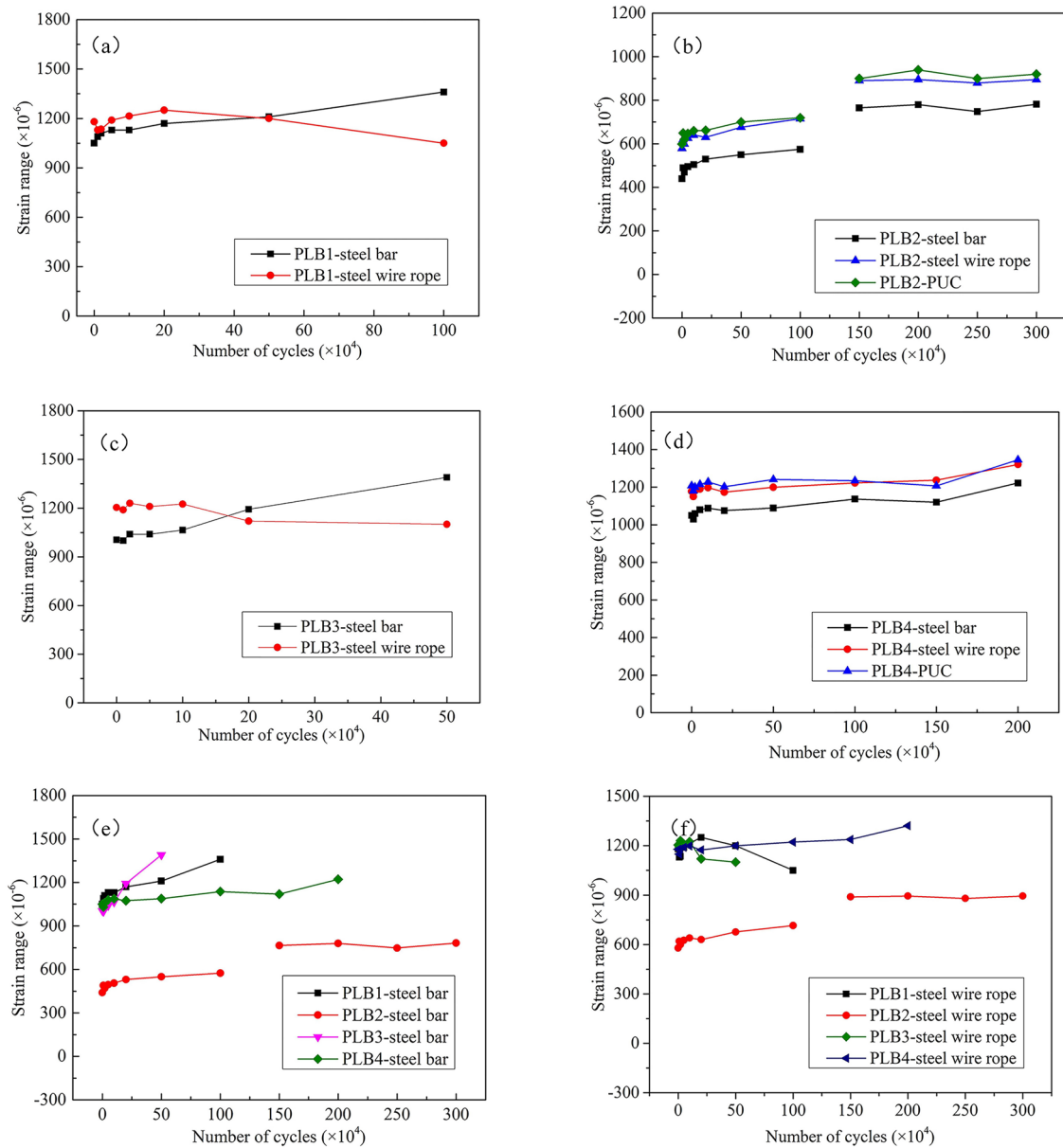


Figure 16: Comparison of strain range in steel bar, PUC, and steel wire rope. (a) Strain range of beam PLB1 under different cycles; (b) Strain range of beam PLB2 under different cycles; (c) Strain range of beam PLB3 under different cycles; (d) Strain range of beam PLB4 under different cycles; (e) Comparison of strain range of steel bar; (f) Comparison of strain range of steel wire rope.

ally decreases. Due to the cracking, falling off, and peeling of polymer mortar, the bonded prestressed wire rope becomes unbonded prestressed wire rope, which redistributes the stress of the beam.

4.4. Static load behavior after fatigue test

After 2,000,000 cycles, beams PLB2 and PLB4 were not damaged. Static load tests were carried out on the two beams to accurately obtain the static properties and residual bearing capacity of the beams after fatigue damage. The yield load of beam PLB2 is 130 kN, which is 5 kN smaller than that of beam B3. The cyclic load has no obvious effect on the strength of beam PLB2. When the load reached 170 kN, the strain of concrete increased more rapidly, and at the same time, the midspan deflection increased more significantly than before. When the load reaches 212 kN, the failure is caused by the fracture of the reinforcement layer, as shown in Figure 17.

The maximum and amplitude of the fatigue load of beam PLB4 are larger than those of beam PLB2. Before 1,500,000 cycles, the cumulative damage of the beam increased, resulting in a significant increase in the mid-span deflection of the beam. The yield load of beam PLB4 is 100 kN, which is 30 kN less than that of



Figure 17: Failure mode of beam PLB2 under static load after fatigue test.

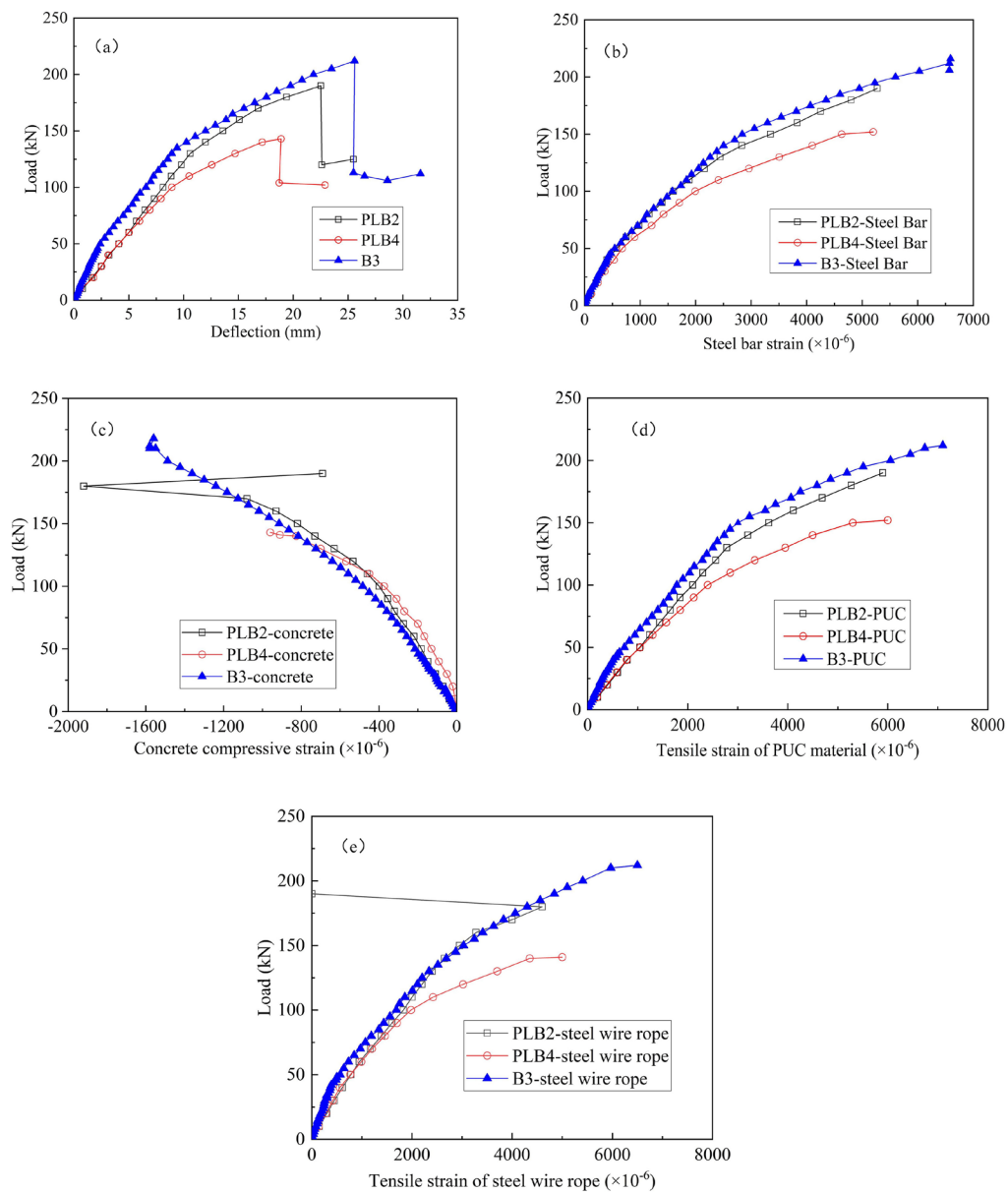


Figure 18: Static behavior of beams PLB2 and PLB4 after fatigue loading. (a) Relation curve between load and midspan deflection; (b) Relation curve between load and steel bar strain; (c) Relation curve between load and concrete compressive strain; (d) Relation curve between load and PUC tensile strain; (e) Relation curve between load and steel wire ropes.

Table 4: Bearing capacity and deflection of PLB2 and PLB4 beams after fatigue testing.

| BEAM NUMBER | YIELD LOAD | ULTIMATE LOAD | YIELD DEFLECTION | ULTIMATE LOAD |
|-------------|------------|---------------|------------------|---------------|
| PLB2 | 130 | 190 | 10.6 | 22.5 |
| PLB4 | 100 | 140 | 8.9 | 18.9 |
| B3 | 135 | 212 | 9.4 | 25.6 |

beam PLB2. When the load reaches 135 kN, the strain of the steel bar and reinforcement layer increases rapidly, and the deflection of the beam increases sharply. When the load reached 140 kN, with a loud bang, the steel bar suddenly broke, and then the reinforcement layer broke.

The performance of beams PLB2 and PLB4 after the fatigue test is compared with that of beam B3 under monotonic loading, as shown in Figure 18 and Table 4. The deflection and strain response of the PLB2 beam is close to those of the B3 beam before steel yield. The yield load of beam PLB2 is only 96% of that of beam B3, while the yield load of beam PLB4 is only 77% and 74% of that of beams PLB2 and B3. Under the action of 140 kN load, the reinforcement layer of the beam PLB4 is damaged first, which is 50 kN less than that of the beam PLB2. The results show that although the maximum load and load amplitude of beam PRF2 is larger than those of beam PRF1 during the fatigue process, leading to more serious damage, there is a small difference between the two beams in the strength degradation of the reinforced layer under cyclic load. After 2,000,000 cycles, beams PLB2 and PLB4 were not damaged. The static performance and residual bearing capacity of the beam after fatigue damage were higher than expected and stronger than those of the PSWR-PM reinforced beam. Moreover, the reinforcement layer did not detach from the bottom edge concrete during the entire loading process, and the PSWR-PUC performance was fully utilized. Reached the industry standard of no delamination or damage to the reinforcement layer after 2,000,000 cycles.

5. CONCLUSIONS

In order to study the fatigue behavior of reinforced concrete beams strengthened by PSWR-PUC, three beams were tested under static load, and five beams were tested under fatigue. The specimens were composed of PSWR-PUC reinforced beams, PSWR-PM reinforced beams, and unreinforced beams. The fatigue performance of beams with different reinforcement techniques was compared during the test. The experimental results show that the monotone loading and fatigue properties of RC beams strengthened by PSWR-PUC are significantly better than those strengthened by PSWR-PM because the deflection and strain of steel bars are significantly reduced by PUC. Similarly, the strain range and maximum strain of the PSWR-PUC reinforced beam are significantly smaller than those of the PSWR-PM reinforced beam under the same load.

With a maximum load of 70 kN and a load range of 40 kN, the PSWR-PM reinforced beam PLB1 was subjected to 1,323,000 loading cycles and failed due to steel fracture. In comparison, the PSWR-PUC reinforced beam PLB2 was subjected to 3,000,000 cycles, with the first 1,000,000 cycles corresponding to a maximum load of 15 kN and a loading range of 40 kN, and the remaining 2,000,000 cycles corresponding to a maximum load of 70 kN and a loading range of 40 kN. In addition, the PSWR-PUC reinforced beam PLB4 survived 2,000,000 loading cycles, corresponding to a maximum load of 95 kN and a loading range of 50 kN, and its reinforcement strain was similar to that of the PSR-PUC beam PLB4.

It is worth noting that the peeling of composite mortar and concrete and the mesh cracks on the surface of composite mortar are observed in the fatigue tests of PSWR-PM reinforced beams. After cracking and peeling of polymer mortar (PM), the tensile strain of reinforcement increases, which exceeds the increase of PSWR strain, indicating that the tensile stress is redistributed between the reinforcement and reinforcement layer. Because of this redistribution, it is considered that the fatigue life of PSWR-PM reinforced beams is relatively short. However, although they were subjected to higher maximum loads and load ranges, the two beams reinforced with PSWR-PUC showed no signs of peeling and cracking of the reinforced layer. The performance of the PSWR-PUC reinforced beam PLB2 shows no obvious degradation after 3,000,000 loading cycles compared to that of the reference beam B3. The reinforcement layer of PSWR-PUC is damaged by cyclic loading. The ultimate load and corresponding PUC strain of the PLB4 beam are 89.6% and 83.1% of that of reference beam B3, respectively. After 2,000,000 cycles under relatively high load and load amplitude, the corresponding loads of steel yield and failure of the reinforcement layer of beam PLB4 are 74.1% and 66% of the reference beam B3, respectively. After 3,000,000 loading cycles, the fracture strain of beam PLB2 reinforced layer is quite close to that of beam PLB4.

6. ACKNOWLEDGMENTS

The authors are grateful for the financial support of the Doctoral Start-up Foundation of Liaoning Province (Project No. 2021-BS-168), the Basic Research Projects of Liaoning Provincial Department of Education in 2024 (Project No. LJ212410153003), and the Shenyang Science and Technology Project Fund (Project No. 23-407-3-19).

7. BIBLIOGRAPHY

- [1] LIU, G.W., OTSUKA, H., MIZUTA, Y., *et al.*, “A foundational study on static mechanical characteristics of the super lightweight and high strength material using fly - ash”, *Zairyo*, v. 55, n. 8, pp. 738–745, 2006. doi: <http://doi.org/10.2472/jms.55.738>.
- [2] HUSSAIN, H.K., ZHANG, L.Z., LIU, G.W., “An experimental study on strengthening reinforced concrete T - beams using new material poly - urethane - cement (PUC)”, *Construction & Building Materials*, v. 40, pp. 104–117, 2013. doi: <http://doi.org/10.1016/j.conbuildmat.2012.09.088>.
- [3] JIA, D.Z., BAO, W.H., JIA, Z., *et al.*, “Preparation and photo - responsive behavior of reversible photo-chromic polyurethane cement composites”, *Applied Physics. A, Materials Science & Processing*, v. 126, n. 5, pp. 1–9, 2020. doi: <http://doi.org/10.1007/s00339-020-03574-7>.
- [4] HUSSAIN, H.K., LIU, G.W., YONG, Y.W., “Experimental study to investigate mechanical properties of new material polyurethane - cement composite (PUC)”, *Construction & Building Materials*, v. 50, n. 15, pp. 200–208, 2014. doi: <http://doi.org/10.1016/j.conbuildmat.2013.09.035>.
- [5] ZHANG, K.X., SUN, Q.S., “Bending fatigue properties research of polyurethane cement (PUC)”, *Civil Engineering Journal*, v. 28, n. 2, pp. 151–160, 2019.
- [6] GAO, H.S., SUN, Q.S., “Study on fatigue test and life prediction of polyurethane cement composite (PUC) under high or low temperature conditions”, *Advances in Materials Science and Engineering*, v. 2020, n. 17, pp. 1–14, 2020. doi: <http://doi.org/10.1155/2020/2398064>.
- [7] ZHANG, K.X., SUN, Q.S., “Strengthening of a reinforced concrete bridge with polyurethane - cement composite (PUC)”, *The Open Civil Engineering Journal*, v. 10, n. 1, pp. 768–781, 2016. doi: <http://doi.org/10.2174/1874149501610010768>.
- [8] ZHANG, K.X., SUN, Q.S., “Experimental study of reinforced concrete T - beams strengthened with a composite of prestressed steel wire ropes embedded in polyurethane cement (PSWR–PUC)”, *International Journal of Civil Engineering*, v. 16, n. 9, pp. 1109–1123, 2018. doi: <http://doi.org/10.1007/s40999-017-0264-x>.
- [9] ZHANG, K.X., SUN, Q.S., “The use of wire mesh - polyurethane cement (WM - PUC) composite to strengthen RC T - beams under flexure”, *Journal of Building Engineering*, v. 15, pp. 122–136, 2018. doi: <http://doi.org/10.1016/j.jobe.2017.11.008>.
- [10] WU, G., WU, Z.S., JIANG, J.B., *et al.*, “Experimental study of RC beams strengthened with distributed prestressed high - strength steel wire rope”, *Magazine of Concrete Research*, v. 62, n. 4, pp. 253–265, 2010. doi: <http://doi.org/10.1680/mac.2010.62.4.253>.
- [11] WU, G., WU, Z.S., WEI, Y., *et al.*, “Flexural strengthening of RC beams using distributed prestressed high strength steel wire rope: theoretical analysis”, *Structure and Infrastructure Engineering*, v. 10, n. 2, pp. 160–171, 2012. doi: <http://doi.org/10.1080/15732479.2012.715174>.
- [12] HUANG, H., LIU, B.Q., XI, K.L., *et al.*, “Interfacial tensile bond behavior of permeable polymer mortar to concrete”, *Construction & Building Materials*, v. 212, pp. 210–221, 2016. doi: <http://doi.org/10.1016/j.conbuildmat.2016.05.149>.
- [13] HUANG, H., HOU, J.L., LIU, B.Q., “Mechanism of debonding failure between reinforced layer with stainless steel wire mesh and polymer mortar and RC structures”, *Advanced Materials Research*, v. 163–167, pp. 3504–3510, 2010. doi: <http://doi.org/10.4028/www.scientific.net/AMR.163-167.3504>.
- [14] LIU, Z.Q., HUA, Q.X., GUO, Z.X., *et al.*, “Test on fatigue behavior of RC bridge girders strengthened with PHSW - PM in moment”, *China Journal of Highways*, v. 31, n. 11, pp. 102–112, 2018.
- [15] ZHANG, K.X., QI, T.Y., ZHU, Z.M., *et al.*, “Strengthening of a reinforced concrete bridge with a composite of prestressed steel wire ropes embedded in polyurethane cement”, *Journal of Performance of Constructed Facilities*, v. 35, n. 5, pp. 04021063, 2021. doi: [http://doi.org/10.1061/\(ASCE\)CF.1943-5509.0001640](http://doi.org/10.1061/(ASCE)CF.1943-5509.0001640).

- [16] ZHANG, K.X., SHEN, X.Y., LIU, J.C., *et al.*, “Flexural strengthening of reinforced concrete T - beams using a composite of prestressed steel wire ropes embedded in polyurethane cement (PSWR - PUC): theoretical analysis”, *Structures*, v. 44, pp. 1278–1287, 2022. doi: <http://doi.org/10.1016/j.istruc.2022.08.014>.
- [17] JIA, Z., JIA, D.Z., SUN, Q.S., *et al.*, “Preparation and mechanical - fatigue properties of elastic polyurethane concrete composites”, *Materials*, v. 14, n. 14, pp. 3839, 2021. doi: <http://doi.org/10.3390/ma14143839>. PubMed PMID: 34300759.
- [18] DING, H.J., SUN, Q.S., WANG, Y.Q., *et al.*, “Flexural behavior of polyurethane concrete reinforced by carbon fiber grid”, *Materials*, v. 14, n. 18, pp. 5421, 2021. doi: <http://doi.org/10.3390/ma14185421>. PubMed PMID: 34576644.
- [19] ZHANG, K., WANG, Y., CAO, D., *et al.*, “Flexural behavior analysis of a composite of high-strength wire mesh and polyurethane cement (HSWM-PUC)”, *Matéria*, v. 29, n. 4, e20240463, 2024. doi: <http://doi.org/10.1590/1517-7076-rmat-2024-0463>.
- [20] CHINESE NATION STANDARDS, *JTG E30-2005 Test method of cement and concrete*, Beijing, Ministry of Communications of PRC, 2005.
- [21] CHINESE NATION STANDARDS, *Method of testing cements - determination of strength*, Beijing, State Bureau of Quality Technical Supervision, 1999.
- [22] CHINESE NATION STANDARDS, *GB/T 5224-2023 steel strand for prestressed concrete*, Beijing, State Administration for Market Regulation and Standardization Administration of China, 2023.
- [23] CHINESE NATION STANDARDS, *GB/T 21839-2019 test methods for steel for prestressed concrete*, Beijing, State Administration for Market Regulation, 2019.
- [24] CHINESE NATION STANDARDS, *GB 50204-2015 code for acceptance of construction quality of concrete structures*, Beijing, Ministry of Housing and Urban-Rural Development of the People’s Republic of China and General Administration of Quality Supervision, Inspection and Quarantine of the People’s Republic of China, 2015.